

Supporting information

Gadolinium-based ultra-small nanoparticles augment radiotherapy-induced T-cell response to synergize with checkpoint blockade immunotherapy

Huijuan Song^{a, ‡}, Hao Sun^{a, ‡}, Ningning He^a, Chang Xu^a, Yan Wang^a, Liqing Du^a, Yang Liu^a, Qin Wang^a, Kaihua Ji^a, Jinhan Wang^a, Manman Zhang^a, Yeqing Gu^a, Yumin Zhang^a, Li Feng^b, Olivier Tillement^c, Weiwei Wang^{d*}, Qiang Liu^{a*}

^a Institute of Radiation Medicine, Chinese Academy of Medical Sciences & Peking Union Medical College, Tianjin 300192, China.

^b Department of Ultrasound, The First Affiliated Hospital of Shandong First Medical University & Shandong Provincial Qianfoshan Hospital, Jinan 250014, China.

^c NH TherAguix, NH TherAguix SAS, Villeurbanne, France.

^d Tianjin Key Laboratory of Biomaterial Research, Institute of Biomedical Engineering, Chinese Academy of Medical Sciences and Peking Union Medical College, Tianjin 300192, China.

* Corresponding authors: Dr. Qiang Liu, E-mail: liuqiang@irm-cams.ac.cn; Prof. Dr. Weiwei Wang, E-mail: wwwangtj@163.com.

‡ These authors contributed equally to this work.

Materials

Fluorochrome-conjugated anti-mouse monoclonal antibodies specific for anti-CD16/32 (clone 93), CD3ε (clone 145-2C11), CD4 (clone GK1.5), CD8 (clone 53-6.7), Foxp3

(clone FJK-16s), Gr-1 (clone RB6-8C5), CD11b (clone M1/70), CD11c (clone N418), CD86 (clone GL-1) were acquired from BioLegend (San Diego, CA, USA). Alexa Fluor 647-conjugated anti-Calreticulin antibody (Catalog: ab196159) was purchased from Abcam (Cambridge, United Kingdom). The mouse regulatory T cell staining kit (clone FJK-16s) was obtained from eBioscience (San Diego, CA, USA). Mouse HMGB-1 (Catalog: SEKM-0145) ELISA kits were received from Beijing Solarbio Science & Technology Co., Ltd. (Beijing, China). The reactive oxygen species assay kit was purchased from Thermo Fisher Scientific (MA, USA). The FITC Annexin V apoptosis detection kit was acquired from BD pharmingen (San Diego, CA, USA). Anti-CD4 (clone GK1.5, Catalog: BE0003-1) and anti-CD8 (clone 53-6.7, Catalog: BE0004-1) antibodies were purchased from BioXCell (NH, USA).

Cell lines and culture

B16 tumor cells (ATCC) were purchased from the Cell Bank at the Chinese Academy of Sciences, and upon receipt, cells were cultured in RPMI 1640 (Gibcol, Grand Island, NY) containing 10% fetal bovine serum (Gibcol, Grand Island, NY), 100 units/mL penicillin and 100 mg/mL streptomycin (Life Technologies, Inc.).

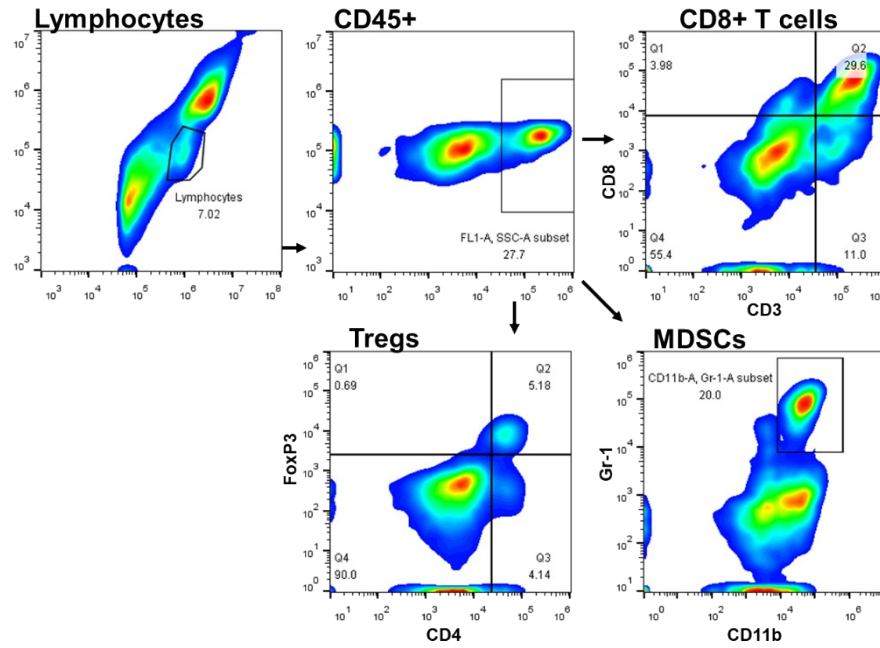


Fig. S1 Representative gating strategies for CD8⁺T cells, T regulatory cells (Tregs) and myeloid-derived suppressor cells (MDSCs) in tumors.

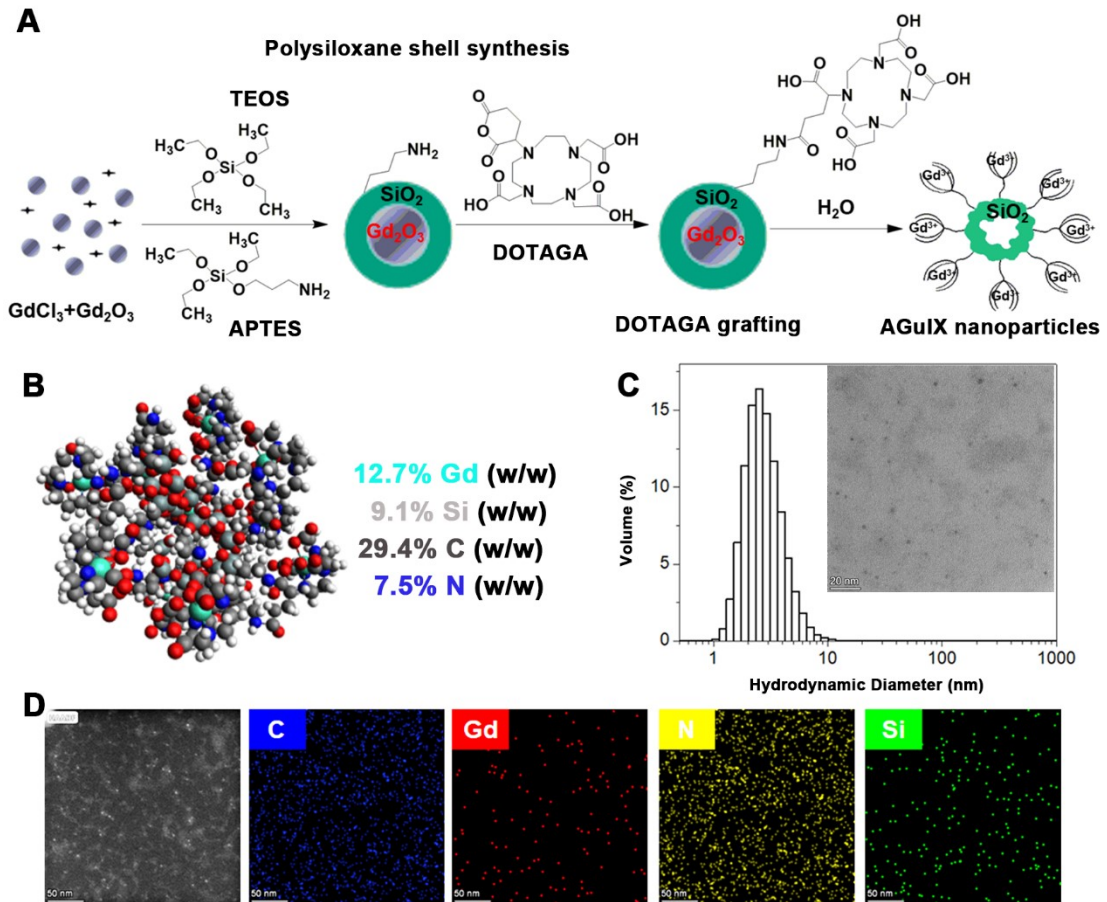


Fig.S2 Preparation route and physicochemical characterization of AGuIX nanoparticles. (A)

Schematic diagram for preparing AGuIX. TEOS: Tetraethyl orthosilicate. APTES: Aminopropyl triethoxysilane. DOTAGA: 1,4,7,10-Tetra-azacyclododecane-1-glutaric anhydride-4,7,10-triacetic acid. (B) Three-dimensional structure and element composition of AGuIX nanoparticles. Gadolinium atoms are represented by green, silicon atoms by pale gray, carbon atoms by gray, nitrogen atoms by blue, oxygen atoms by red, and hydrogen atoms by white color. AGuIX were composed of 12.7% Gd (w/w), 9.1% Si (w/w), 29.4% C (w/w), and 7.5% N (w/w). (C) Volume-weighted particle size distribution of AGuIX nanoparticles determined by dynamic light scattering. The inset shows the transmission electron microscope image of AGuIX particles. (D) EDS elemental mapping of AGuIX nanoparticles.

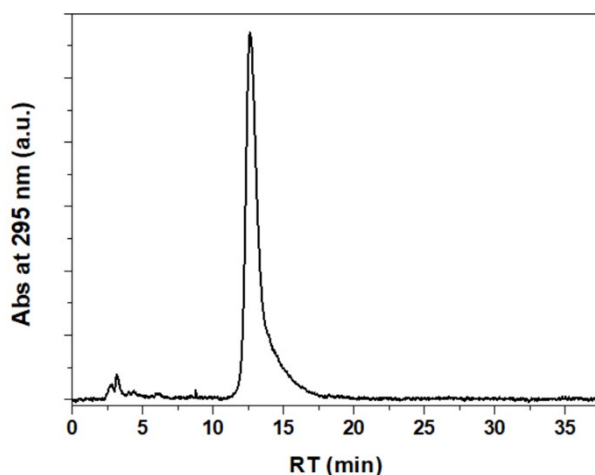


Fig. S3 HPLC measurement of AGuIX nanoparticles (detection at 295 nm).

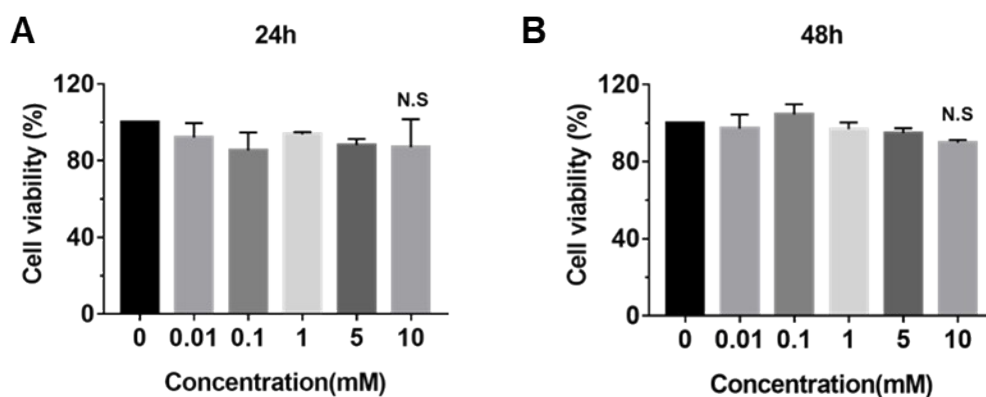


Fig. S4 Cytocompatibility of AGuIX against MRC5 cells *in vitro*.

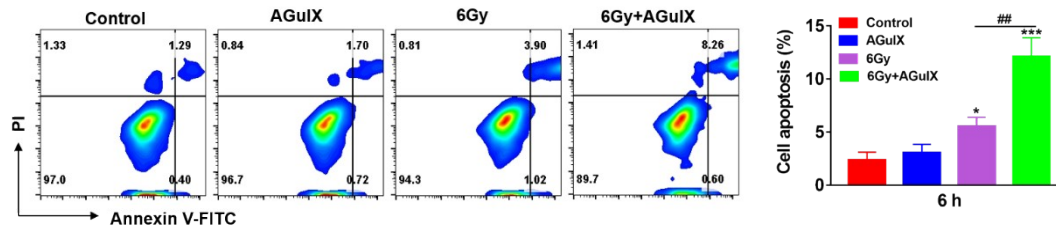


Fig. S5 Annexin V/PI analysis of B16 cells. Qualitative flow cytometry data plot showing the increased apoptosis caused by the AGuIX nanoparticles under irradiation, 6 h postirradiation.

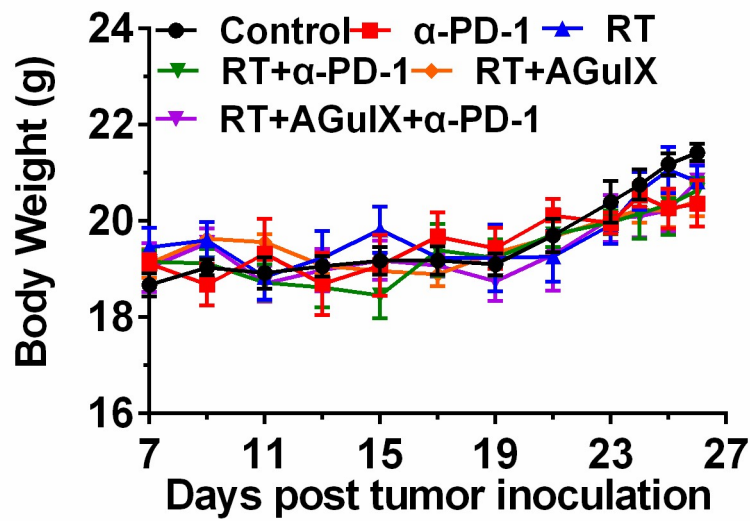


Fig. S6 Mouse body weight growth curve.

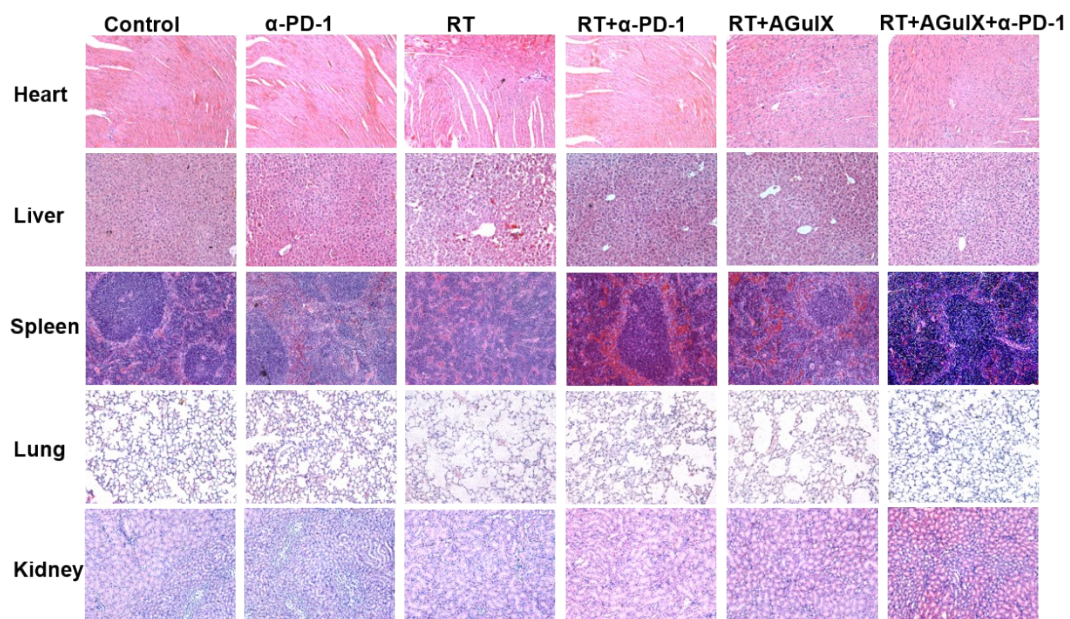


Fig. S7 H&E staining of the collected organs from different groups.

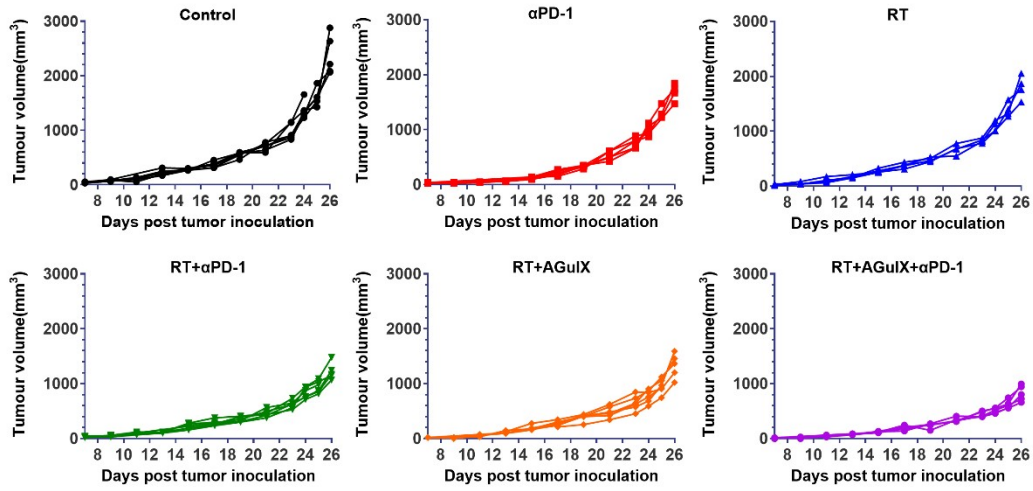


Fig. S8 Profile of tumor volume in each group of mice.

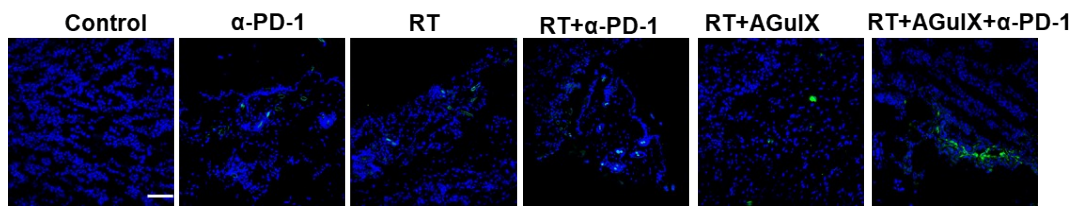


Fig. S9 Expressions of perforin in tumor tissues after various treatments.

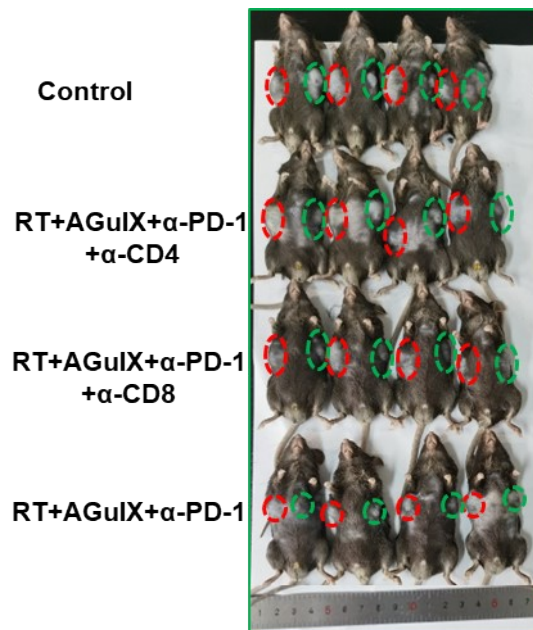


Fig. S10 Tumor photographs of the tumor-bearing mice at the end of the experiment. Primary tumors were represented by red and distant tumors by green color.

